

PROCEEDINGS OF THE
**31st IEEE CONFERENCE ON
DECISION AND CONTROL**

DECEMBER 16-18, 1992
WESTIN LA PALOMA
TUCSON, ARIZONA, USA



IEEE
Control
Systems
Society

VOLUME 2 OF 4

92CH3229-2

Parameter Identification of Large Spacecraft Systems Based on Frequency Characteristics *

Donald R. Augenstein,[†] John S. Baras[‡] and Shalom M. Fisher[§]

Electrical Engineering Department and
Institute for Systems Research
University of Maryland
College Park, MD 20742

Abstract

In this paper we describe parameter identification for an in-orbit satellite. Actual experimental results are described for the Low Atmospheric Control Experiment (LACE) spacecraft. This is a low earth orbit satellite that was launched into a circular orbit. Its structure consists of a central rigid body or bus with three deployable booms. We accomplished the identification of the structural modes and damping factors of the spacecraft in orbit utilizing the frequency characteristics of the Hankel operator. Frequency domain error bounds and time domain error bounds were considered. The experiment utilized ground based laser illumination and identified three of the lowest vibration modes. The accuracy of the methods was extremely good.

1. Introduction

The subject of spacecraft structural parameter identification has gained recent attention. With the development of a permanent manned space facility in the near future, the application of sophisticated identification experiments geared to space structures has increasingly become important. Crucial applications of parameter identification of large spacecraft structures are in moni-

toring structural health and control/structure interactions. Structural identification of the spacecraft in its "true" environment will provide confidence in analytical models and hopefully point to areas where more research is needed. In-flight modeling is a major step toward the goal of real-time adaptive attitude control and stabilization.

Recent tests have been done by the US Air Force that tested structural modes on a boom while in the zero-gravity environment of the hold of an airplane in a parabolic dive. A complete deployable solar array experiment was performed in the hold of the space shuttle in 1985 (SAFE). The SAFE experiment used accelerometers attached at the end of the array. Its excitation force was provided by pulsing the space shuttle's thrusters.

2 Experiment Description

The experiment is to measure vibration of the complete spacecraft structure and calculate the system modal frequencies and damping factors.

2.1 Spacecraft Configuration

The experiment was designed for the Low Power Atmospheric Control Experiment (LACE) spacecraft. It is a low earth orbit satellite that was launched on February 14, 1990 into a 540 km altitude circular orbit of 43° inclination orbit. The LACE spacecraft structure is composed of a central rigid body or bus with three deployable booms (See Figure 1). The bus carries the mission primary sensors and experiments, all supporting telemetry/command modules, attitude and control subsystem and the solar panels.

*Research supported in part by NSF grant NSFD CDR8803012.

[†]The author was with the Systems Research Center, University of Maryland, he is now with MPR Associates Inc., Washington, DC.

[‡]Martin Marietta Chair in Systems Engineering.

[§]Naval Research Laboratory, Washington, DC.

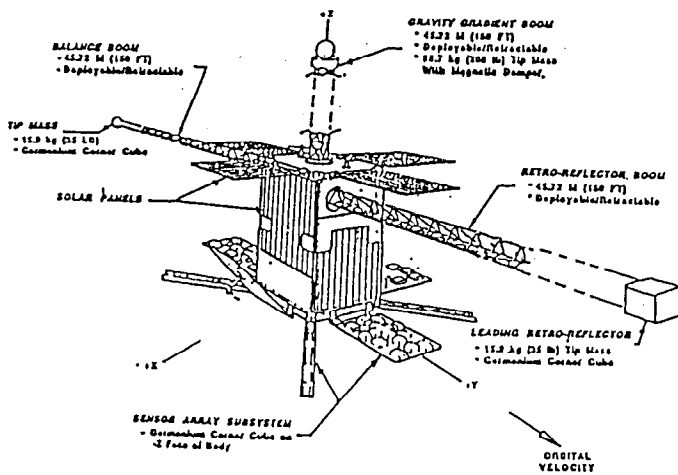


Figure 1. Spacecraft Configuration

Each of the deployed booms has a different mission function. The first boom is the gravity gradient boom and is oriented directly away from the earth. It has an electro-magnetic energy dissipating unit located at the tip. The energy dissipation unit is part of a passive attitude stabilization system that dumps destabilizing dynamic energy using the earth's magnetic fields.

The second boom is the retro-reflector boom and is deployed in the direction of the spacecraft velocity vector. The retro-reflector boom tip has a laser reflector unit mounted on it. Amongst these reflectors is a germanium reflector (approximately 1 inch diameter) that is dedicated to this structural dynamics experiment.

The third boom is the balance boom and is oriented 180 degrees from the retro-reflector boom. The balance boom has a strictly passive role of counteracting the rigid body dynamics due to the retro-reflector boom. The rigid body and the balance boom also have germanium reflectors mounted upon them.

The spacecraft booms are both deployable and retractable. The deployed length varies from 0 feet up to 150 feet. The booms' continuous longerons and stiff cross elements are constructed of light weight composite fiberglass/epoxy material. Given that the boom lengths are variable, the system vibration modes are variable as well and are a function of the deployed length. The booms' undeployed portion remains elasti-

cally coiled in the deploying canister mounted to the main spacecraft body. Additionally, the deploying canister has an elastic compliance. This compliance is incorporated in the vibration analysis, see Table 1. The rigid central body has a mass of 1177 kilograms with moments and products of inertia listed in Table 2. These properties were experimentally measured. The tip masses on each boom are listed in Table 3

density unit kg/m	bending stiffness (EI) N-m ²	torsional stiffness (GJ) N-m ²	Rotating Inertia I_0 unit/length N/sec ²	boom canister compliance N/radian
0.291	$\approx 1.55 \times 10^4$	631	2	1.695×10^4

Table 1: Boom Structural Properties

Inertia	kg - m ²
I_{xx}	1448.7
I_{yy}	1426.4
I_{zz}	1026.2
I_{xy}	3.61
I_{xz}	19.98
I_{yz}	14.86

Table 2: LACE Bus Inertial Properties

boom	kg
Gravity	90.7
Retro-reflector	15.9
Balance	15.9

Table 3: LACE Boom tip masses

3 Experiment Design

The vibrations are generated by the retraction of a retro-reflector boom from 24.384m (80 ft) to 4.572m (15 ft). This type of excitation is due to two factors. The first is the nonlinear coupling of elastic strains of the boom in its canister. The second is due to the lead tip mass being offset from the axis of the boom. This offset creates a moment at the boom tip which excites vibration. While the excitation forces involved are nonlinear, the resulting low level vibration will be within the linear range.

Because the LACE spacecraft does not have telemetered data which can directly indicate the presence of vibratory motion, the measurements were taken indirectly by using remote laser sensing. This technique uses a ground based laser to illuminate the germanium mirrors located on

the spacecraft bus and booms. A reflected laser signal will have a Doppler shift due to the relative motion of the spacecraft with respect to the laser source. The Doppler shift from each of the illuminated mirrors is used to calculate this relative motion. The laser radar operates at a peak transmit power of 800 watts, with pulse duration of 3.4 ms, and sampling at 1.2 MHz. The Doppler resolution is about 294 Hz, giving velocity resolution of 1.8 mm/sec.

In addition to the vibration motion, the Doppler shift will include the rigid body motion of the satellite's orbital motion. This motion is the dominant component of the detected Doppler shift as seen from an earth base observation line of sight vector. Considering that observation windows are short, elimination of this rigid body component is necessary in order to resolve the lowest vibration frequency mode [7].

4 Spacecraft Models

The reference values for the identification results are the modal frequencies calculated from the structural characteristics of the spacecraft. The modal analysis is performed using two techniques. The first technique is finite element modeling (FEM), and the second technique is a continuum approach through a partial differential equation model (PDE). The LACE geometry modeling lends itself to straightforward PDE solution. Thus formulated, the solution of the PDE provides a quick and accurate solution. FEM also provides convenient three dimensional modeling, and its results will converge to PDE solutions only as the number of nodes becomes large.

4.1 Euler Beam Model

The basic structural model used was the Euler beam. More complicated models may provide higher "accuracy", however they introduce nonlinear components. While the assumptions justifying the use of an Euler beam model may be severe, they are essentially obeyed considering the small excitation due to the boom retraction. The booms are assumed to be cylindrical beams.

The PDE model used to describe the flexible motion of the beam through any axis is as follows:

$$\frac{\partial^2 w(z,t)}{\partial t^2} + EI \frac{\partial^4 w(z,t)}{\partial z^4} = 0 \quad (1)$$

This equation assumes the material stiffness EI and mass per unit length ρ are uniform along the beam. The values for EI and ρ used in this equation are the same as those in Table 1.

Likewise, the torsional partial differential equation is described by:

$$I_o \frac{\partial^2 \theta(z,t)}{\partial t^2} + GJ \frac{\partial^2 \theta(z,t)}{\partial z^2} = 0 \quad (2)$$

This equation assumes the torsional stiffness GJ and rotating mass inertia per unit length I_o are consistent along the beam. The values for GJ and I_o used in this equation are the same as those in Table 1.

4.2 Modeled Modal Frequencies

Using the model of the previous section, the modal properties of the LACE spacecraft were determined. The spacecraft boom length configuration analyzed was the same as the spacecraft's at the time of the experiment (retro-reflector boom at 15ft, gravity-gradient boom at 150ft, and the balance boom at 150ft).

The projection of the boom tip velocity onto the earth observer's line of sight is normal to all vibration except the pitch plane. Thus, the pitch modes are the only modes that are detectable. In Table 4 the pitch modes below one Hertz are listed. Additionally, Table 4 lists the relative magnitude of displacement experienced at the lead tip for each mode. Relative displacement is the ratio of tip deflection to peak deflection. This ratio gives some insight to which modes are most likely to be detected with the ground based laser. It should be noted that the vibration mode at .7567 Hz is primarily due to the modeled spring compliance of the boom canister. Changing the boundary condition at the spacecraft to a fixed clamp changes this mode.

PDE hz	FEM hz	Displacement Ratio
.01908	.01906	0.0242
.1298	.12981	0.0063
.2581	.25782	0.0284
.3238	.32333	0.0565
.7567	.74952	0.4669
.8217	.81880	0.1068

Table 4: LACE System Pitch vibration modes below 1 Hertz

4.3 Identification Techniques

Since the form of the excitation or driving function cannot be accurately modeled, the analysis is limited to post-excitation free-decay measurements. Additionally, the observable measurement windows available for laser reflections are extremely limited in time and maybe corrupted by noise. Given these limitations, the identification analysis must be robust in the presence of significant noise and must converge to a model given only a small window of measurements. Analysis has shown that identification using the frequency characteristics of the Hankel operator is the best suited for this experiment.

The system modeling duplicates the structural internal dynamics with an impulse response model. The identification utilizes linear system realization theory which provides error bounds on the model's performance. The performance criteria that is considered is the frequency domain L_∞ norm. The Hankel operator algorithms utilized were the eigensystem realization algorithm (ERA) suggested by Juang *et al* [5] and the minimum model error (MME) suggested by Mook *et al* [1].

4.3.1 Model Reduction Algorithm

It was proven independently by Glover(1984) and Enns [3] using optimal Hankel norm approximations that L_∞ norm of the difference between the n^{th} order true system $G_n(s)$ and the internally balanced truncated k^{th} order model $\hat{G}_k(s)$ has the following bound.

$$\| G_n(s) - \hat{G}_k(s) \|_\infty = \sup_{w \in (-\infty, \infty)} | G_n(jw) - \hat{G}_k(jw) | \leq 2 \sum_{i=k+1}^n \sigma_i \quad (3)$$

The following engineering results may be deduced from the balanced order model reductions.

1. The spirit of balanced order truncations is that the least observable and controllable modes are the ones being truncated.
2. The L_∞ bound is significant if $\sigma_k \gg \sigma_{k+1}$ and σ_{k+1} is small. This implies that the sum of the tail of singular values is small and thus the L_∞ bound is tight.

3. The truncations can perform well, even when σ_{k+1} is close to σ_k . Glover (1984) showed this could be true, since as $\sigma_{k+1} \rightarrow \sigma_k$ the poles of the truncation can approach the imaginary axis.
4. If the realization (A, B, C) was constructed from noisy Markov parameters, and if an estimate of the noise variance exists, then a comparison of the L_∞ bound and the noise power spectrum is useful. Given a noise power spectrum:

$$\Phi_{noise}(w) = \sum_{-\infty}^{\infty} R_{noise}(\tau) e^{-irw}$$

if the L_∞ bound satisfies:

$$2 \sum_{i=k+1}^n \sigma_i \approx \sup_w | \Phi_{noise}(w) |$$

then the effect of the truncation is limited to the removal of modes that model the noise contributions.

4.4 Measuring the Distance Between Truncated Systems and Infinite Systems

Curtain *et al* [6] quantified the effects of truncating the infinite Hankel operator matrix to a finite order matrix. Let Γ_n represent the n^{th} order approximate to the complete Hankel operator Γ . Of interest is the size of appropriate norms on the difference between the truncated and infinite operators $\| \Gamma - \Gamma_n \|$. In order to measure the effects of truncating an infinite Hankel operator, Curtain *et al* showed that if the system impulse response $h(t) \in L_1 \cap L_2$ and the Hankel operator was nuclear, then the truncation of the Hankel operator will converge to the true Hankel operator as the order n gets large. Nuclearity is dependent on the system under study. It was shown by de Vries [2] that a system constructed via the Laplace transform of a partial differential equation model of a deployed spacecraft essentially equivalent to the LACE spacecraft is in fact nuclear. A necessary assumption is that the booms have viscous damping. This assumption is quite reasonable since the structural damping factor tested on ground was greater than 1 percent. Additionally, any damped structural system is definitely an element of L_1 . Thus, the assumption of nuclearity is reasonable.

5. Analysis of Experiment with LACE Spacecraft

The experiment yielded four observation windows. Of these windows, only two windows observed the Doppler returns while the spacecraft was in free-decay vibration, days 91008 and 91010. Currently, these two sample periods are the sole periods used in this structural identification process.

The first observation period captures the dynamic motion of the lead boom while the boom is being retracted and immediately following the end of retraction. The second observation period was taken after the retraction was completed. Since there is a delay in the measurement collection, the higher modes will have decayed more. Fortunately, this observation window is much longer.

In addition to the vibrational motion, there is the rigid body motion of the spacecraft due to the change in the ground observer's aspect angle. The apparent change effects the observed Doppler shifted laser return. The effects of this apparent motion are adjusted for by calculating orbital position with respect to the observation site and calculating the apparent motion. The calculated rigid body motion was subtracted from the observed motion. Then the change in aspect angle was corrected.

The PSD of the data sets, sampled in-phase and quadrature, was filtered so as to detect the relative and vibrational motion of the spacecraft. The test data had Doppler shift measurements collected at a 62 Hz sample rate. This rate is significantly higher than the modes of interest. To filter out some of the noise present, groups of 5 samples are taken and the median value of the population is selected. This technique reduces the sample rate to 12.4 Hz, which is more than adequate for analysis.

Using this data, an initial analysis was performed. All the data was initially filtered to eliminate high noise components. Based on analysis of the detected motion PSD, the cutoff frequency was chosen to be .75 Hz. This number allows for decimation in time and is sufficiently separated from the higher modes. The data sets were then decimated in time into distinct data sets. Each of these data sets were then analyzed and statisti-

cally compared. Tables 5 through 8 show details from the results of this study.

The results of this analysis are quite impressive. Given such short observation windows, the algorithms detected modes which correlate well with predictions. Four vibration modes were detected on day 91010, of which three were among the first four pitch plane vibration modes. Three vibration modes were detected on day 91008, of which two were among the first four pitch plane vibration modes.

Both observation days detected a mode not previously predicted by the PDE or FEM models. This moderately damped mode at $\approx .52$ Hz is probably not due to the boom elements because the damping is too high. While the explanation for this mode is yet unknown it is believed to be due to either unmodeled behavior within the boom canisters or vibrations that are due to the cantilevered retro-reflector plate. Such elastic behavior would tend to be nonlinear and will have higher damping. Its damping factor was between 5 and 11 percent. This level is significantly higher than the other modes.

The identified modes were within .005 to .01 Hz of the predicted modes depending on the identification technique compared. While this is impressive, the identification of the damping factors had a larger variance. This variance is due to the fact that the period of observation was very short in comparison to the period of the mode which causes the parameter identification to be more sensitive to noise. In the future, longer observation windows will provide enough information to get better damping calculations.

Model Mode Hz.	ERA Hz.	std. dev. Hz.	ERA/MME Hz.	std. dev. Hz.
0.1298	0.1225	0.0005	0.1226	0.0005
.3238	0.3245	0.0003	0.3248	0.0006
	0.5219	0.0025	0.5201	0.0030

Table 5: Day91008 Identification Results: Modal Frequencies

Model Mode	ERA %	std. dev.	ERA/MME %	std. dev.
0.1298	-0.1244	0.2489	-0.3518	0.3027
0.3238	1.4477	0.0410	1.1137	0.0473
	4.8917	0.2984	4.5929	0.2631

Table 6: Day91008 Identification Results: Damping Factors

Model Mode Hz.	ERA Hz.	std. dev. Hz.	ERA/MME Hz.	std. dev. Hz.
0.0191	0.0208	0.0033	0.0210	0.0020
0.1298	0.1244	0.0010	0.1245	0.0011
0.3238	0.3312	0.0009	0.3320	0.0008
	0.5115	0.0061	0.5120	0.0064

Table 7: Day91010 Identification Results: Modal Frequencies

Model Mode	ERA %	std. dev.	ERA/MME %	std. dev.
0.0191	1.8385	1.8277	1.3937	2.260
0.1298	2.3233	0.5182	2.1029	0.3007
0.3238	2.1114	0.2312	2.0058	0.2971
	10.4537	1.2157	10.7973	1.0233

Table 8: Day91010 Identification Results: Damping Factors

6 Conclusions and Interpretations

Considering the brevity of the observation windows, the experiment was extremely successful. The experiment accomplished the following goals.

Structural modes were verified independently using the actual spacecraft in its true environment. Three of the first four modes were detected. These results are impressive compared to previous experiments, specifically, the 1985 Solar Array Flight Experiment (SAFE). The SAFE experiment, which was a two day experiment done on board the space shuttle, tested the modal properties of a deployed truss with an attached solar panel. It only detected three modes.

Algorithms were tested with an actual experiment and provided robust identification. The

identified modes were tightly grouped and agreed with predicted modes. The Hankel operator technique performed best.

A new laser application was verified. This experiment showed that laser tracking could be accomplished and provide data on which analysis could be performed. This approach offers alternative experimental approaches to structural identification for low orbit satellites.

References

1. D. J. Mook, J. L. Junkins. Minimum Model Error Estimation for Poorly Modeled Dynamic Systems. *AIAA Journal of Guidance, Control, and Dynamics*, 11(4):365-375, May-June 1988.
2. S. A. de Vries. Frequency domain analysis of models of flexible beams. Master's thesis, University of Groninge, 1988.
3. D. Enns. *Model reduction for Control system Design*. Ph.D. thesis, Stanford University, 1984.
4. Glover, K. All-optimal Hankel-norm approximations of Linear multivariable systems and their L_∞ error bounds. *International Journal of Control*, 39:1115-1193, 1984.
5. J. N. Juang, R. S. Pappa. An Eigensystem Realization Algorithm (ERA) for Modal Parameter Identification and Model Reduction. *AIAA Journal of Guidance, Control, and Dynamics*, 8(5):620-627, Sept.-Oct.1985.
6. K. Glover, R. Curtain, and J. Partington. Realization and Approximation of Linear Infinite-Dimensional systems with Error Bounds. *SIAM Journal of Control and Optimization*, 26(4):863-898. July 1988.
7. K. I. Schultz. Analysis of narrowband IR LACE measurements acquired during GMT days 195 and 200. MIT Lincoln Laboratory Memo, August 1990.